Indonesian Journal of Science & Technology

The Ship's Propeller Rotation Threshold for Coral Reef Ecosystems Based on Sediment Rate Indicators: Literature Review with Bibliometric Analysis and Experiments

Abdul Kadir [1,2,], I. Istadi[1], Agus Subagio[1], W. Waluyo[2], Abdul Muis[2]*

[1]Universitas Diponegoro, Semarang 50275, Indonesia
[2]National Research and Innovation Agency (BRIN), Jakarta 10340, Indonesia
*Correspondence: E-mail: abdkptrim@students.undip.ac.id

A B S T R A C T

The rotation of ship propellers produces water flows that can trigger erosion and resuspension of sediment on the seabed, which damages coral reef habitats. The causal relationship between propeller rotation and coral reef damage must be known to obtain the necessary environmental constraints. This research uses bibliometric analysis and experiments to determine safe propeller rotation thresholds based on sediment rate indicators. The water flow velocity from the propeller rotation was measured through experiments in various rotations. The sedimentation rate is determined using empirical calculations based on the water flow velocity value. The analysis results determine that the rotation threshold for a propeller diameter (*Dp*) of 1.5 m is: (a) 120 rpm if the vertical position of the propeller axis is 0.5*Dp* above the seabed; (b) 230 rpm if the vertical position of the propeller axis is 1.0*Dp* above the seabed; and (c) 360 rpm if the vertical position of the propeller axis is $\geq$ 1.5Dp above the seabed. The results of this research become a benchmark for the environmentally friendly operation of ship propellers.

A R T I C L E   I N F O

1. INTRODUCTION

In the last five years, the number of ship visits at all Indonesian ports has reached an average of 820,000 per year, as seen in **Table 1**. This achievement is hoped to continue to increase, considering its significant influence on Indonesia's economic growth as an archipelagic country.

Table 1. Number of voyage ship calls at all ports of Indonesia (in units).

Year	Domestic Voyage	International Voyage	Total of Voyage Ship Call
2018	745,627	83,646	829,273
2019	806,189	89,339	895,528
2020	658,753	56,918	715,671
2021	711,240	42,090	753,330
2022	830,027	64,453	894,480

However, this condition can hurt coastal water ecosystems through the pollution it causes. There are at least 13 types of pollution that can be caused by ships, including antifouling paint, ballast water, bilge water, biofouling, waste, grey water, food waste, scrubber water, stern oil, underwater noise, engine exhaust, anchors and moorings can damage and disturb marine biota (Ytreberg *et al.,* 2021; Forrester, 2020; Flynn & Forrester, 2019).
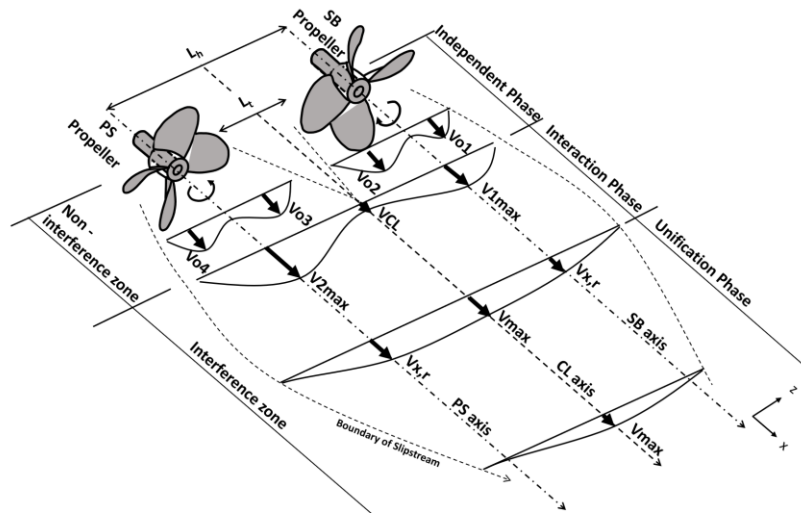
Several studies concluded that ship propeller rotation can cause seabed damage through sediment resuspension (Kaidi *et al.,* 2021). Erosion and sedimentation from shipping activities raise the shallowing in port areas (Guarnieri *et al.,* 2021; Scully & Young, 2021). Besides that, sediment particles will cover coral organisms reduce light levels, inhibit photosynthesis, and affect the structure and function of coral reef ecosystems through physical and biological processes (Rogers, 1990). Mud and sedimentation will kill young coral, resulting in degradation (Victor *et al.,* 2006). Increased sediment supply to coral reef ecosystems and other influencing factors will endanger coral reef health (Ryan et al., 2008). Increased fine sediment causes constriction and accumulation of coral polyps, shading, tissue necrosis, and increased bacterial populations in coral mucus (Erftemeijer *et al.,* 2012).

Damage to coral habitat due to sedimentation caused by shipping activities, land pollution, and coastal development also occurs in Indonesia (Ceccarelli *et al.,* 2022). From 1990 to 2020, Indonesia restored the condition of damaged corals in 533 locations (Razak *et al.,* 2022). Currently, the government conserves around 569 coral species, or almost 69% of the total global coral species. The government is very concerned about preserving coral reefs, considering that coral reefs are spread over approximately 39,538 km² or the equivalent of 16% of Indonesia's world's coral reef area.

Research on sedimentation due to ship propeller rotation has yet to be connected to the impact of sedimentation on coral reef habitats. The gap between the two fields can be identified through searching research records with bibliometric data analysis. Bibliometric analysis helps produce network visualization of co-work maps and co-work density maps among research results (Al Husaeni & Nandiyanto, 2022). The systematic steps of bibliometric analysis have been widely applied to research in various fields, such as bibliometric analysis of Indonesian journal research materials using VOSviewer (Nandiyanto & Al Husaeni, 2021), the field of bioenergy management (Soegoto *et al.,* 2022), and the field of statistics and engineering (Fiandini *et al.,* 2024).

An essential factor that needs to be considered when using a bibliometric system is keywords related to the research object. Some keywords used for this research are ship

propeller rotation, erosion and sedimentation, coral reef habitat, aquatic ecosystems, and port environments. A literature search was conducted based on keywords regarding research conducted between 2013 and 2023. No research was found regarding the direct impact of sedimentation caused by propeller rotation on coral reef damage.

Figure 1 depicts a network of research collaborations in various interrelated fields. The size of the notation describes the intensity of the research carried out, where the more significant the notation, the more research is carried out in that field. Based on the description of the research network, it can be seen that four areas form central nodes, namely propellers, shallow waters, sedimentation, and coral reefs. There is still a gap between the four research areas, and one is that ship propeller rotation is not directly connected to research on damage to coral reefs due to sedimentation.

Based on the existing gaps, this research aims to determine the threshold for propeller rotation that causes sedimentation that does not damage coral reef life. The results of this research are essential input for the government in developing environmentally friendly ship operating regulations, primarily to protect coral reef ecosystems.

Figure 1. The field research gaps.

2. LITERATURE REVIEW
2.1. The Erosion and Sedimentation Posture of the Twin-propeller Rotation

Figure 2 explains the water flow velocity pattern in the twin-propeller. Each propeller forms two peak speeds between its rotational axes in the non-interference zone. This zone is also called the free phase, where the flow velocity of the two propellers does not influence each other, so a single propeller system approach applies. In the interference zone, the two water flows interact on the center line axis, so the twin-propeller approach applies. In the interaction phase, the combined speed of the water flow forms two speed peaks, but at a certain distance, it will change to form one peak on the centerline axis between the two propellers. This condition is called the unification phase.

Figure 2. The water flow zone of the external counter rotating of the twin propeller (*ECRTP*).

Erosion and sedimentation processes begin to occur when the water flow velocity from the propeller rotation causes the bottom shear stress (θ) to be greater than the threshold value (θcr) (Van Rijn, 2007). The shear stress value depends on the type of particle and grain diameter.

Several previous studies have discussed the erosion and sedimentation postures of both single-propeller and twin-propeller rotation, wherein a twin-propeller the posture of erosion and sedimentation is determined by the type of propeller rotation used (Tan & Yüksel, 2018; Penna *et al.*, 2019; Cui *et al.*, 2019a; Cui *et al.*, 2020; Curulli *et al.*, 2022; Curulli *et al.*, 2023). The external Counter Rotating Twin Propeller (*ECRTP*) is a rotating system on a double propeller with a scouring posture, as shown in **Figure 3**.

(a) Side and Plan view   (b) Cross section (A'- A')
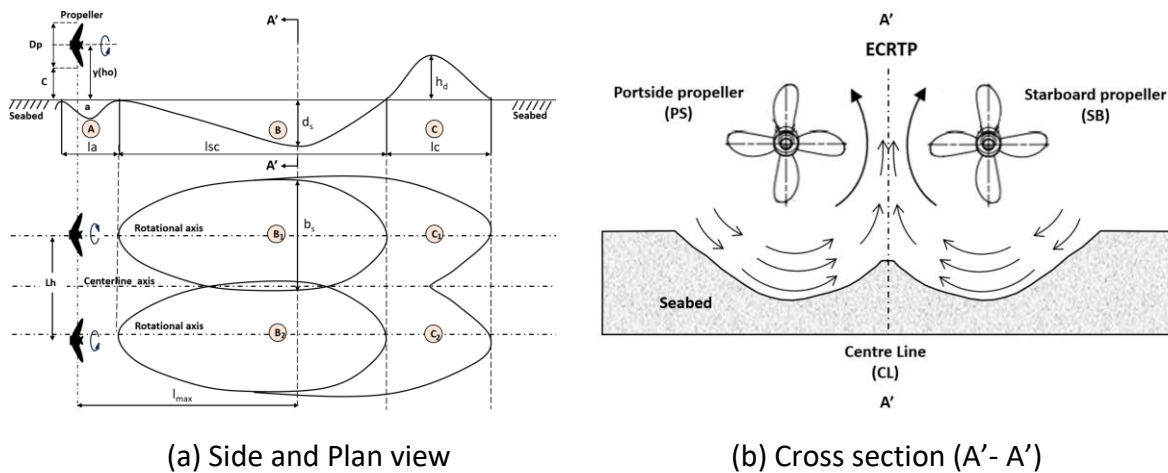
Figure 3. Scour posture of ECRTP is referred to (Cui 2019; Cui *et al.*, 2019a).

Based on **Figure 3(a)**, it can be explained that the scour produced by each propeller consists of part (A) of small scours under the propeller. Long blades (*a*) tend to avoid sedimentation so that they can be ignored in calculations; part (B) is the main scour on the seabed with maximum scour length (*lsc*), maximum depth (*ds*), and maximum width (*bs*). This section is a scour that produces many sediment particles, most of which will settle near the scour hole, and some of the particles will be carried by the water flow and settle in further places; part (C) is a pile of sediment deposits with maximum pile height (*hd*). The scoured area and scoured volume are symbolized as (*As*) and (*Ve*), respectively.

The horizontal distance between the propeller center point and the depth maximum can be determined by referring to the Eq. (1) (Tan & Yüksel, 2018):

$$l_{max} = Fr_d^{0.724} G^{0.09} D_p^{0.91} \tag{1}$$

where G equal to h_o is the distance from the propeller axis to the bottom, Dp is the propeller diameter, Fr_d is the Froud Number densimetry from the equation $Fr_d = U_0 / \left((gd_{50}(\rho_s - \frac{\rho}{\rho}))^{0.5} \right)$, U_0 is the water flow axial velocity, g is gravity acceleration, d_{50} is the median diameter of the particle, ρ_s is the specific weight of the sediment, ρ is the specific weight of the fluid.

Figure 3(b) shows the transverse scour posture, where it can be seen that the scour that occurs from each propeller rotation does not coincide with the others. Thus, the single propeller calculation principle can be used for each propeller.

Scour dimensions, area, and volume can be determined through the Eqs. (2) – (7) proposed by Cerulli (Curulli *et al.*, 2023):

Scour length (l_{sc}) is shown in Eq. (2):

$$\frac{l_{sc}}{D_p} = 10.16 F_{0p} \left(\frac{d_{50}}{D_p} \right)^{0.03} \tag{2}$$

where F_{0p} is the propeller Froude number from the equation $F_{0p} = U_0 / (gD_p)^{0.5}$

Scour width (b_s) is shown in Eq. (3):

$$\frac{b_s}{D_p} = 4.61 F_{0p}^{0.83} \left(\frac{d_{50}}{D_p} \right)^{-0.03} \left(\frac{h_0}{D_p} \right)^{-0.44} \tag{3}$$

where h_0 is the distance from the propeller axis to the base.

Scour depth (d_s) is shown in Eq. (4):

$$\frac{d_s}{D_p} = 0.90 F_{0p}^{1.30} \left(\frac{d_{50}}{D_p} \right)^{-0.05} \left(\frac{h_0}{D_p} \right)^{-0.53} \tag{4}$$

Sediment stack height (h_d) is shown in Eq. (5):

$$\frac{h_d}{D_p} = 2.29 F_{0p}^{1.48} \left(\frac{d_{50}}{D_p} \right)^{0.13} \left(\frac{h_0}{D_p} \right)^{-1.25} \tag{5}$$

Scour area (A_s) is shown in Eq. (6):

$$\frac{A_s}{D_p^2} = 0.52 \left(\frac{l_{sc} b_s}{D_p^2} \right)^{1.16} \tag{6}$$

Sediment scour volume (V_e) is shown in Eq. (7):

$$\frac{V_e}{D_p^3} = 0.53 \left(\frac{l_{sc} d_s b_s}{D_p^3} \right)^{0.95} \tag{7}$$

2.2. Sedimentation Rate

Sediment deposits from floating sediments can be determined based on the sedimentation rate in (mg/cm^2.d) units. The rate of fine sediment deposition is generally around $25 - 50$ m/d or equivalent to $0.03 - 0.06$ cm/s. By applying the principles of Stokes' law, the terminal velocity of falling particles can be determined by the Eq. (8).

$$v = \left(\frac{2}{9} \frac{r^2 (\rho_s - \rho_f)g}{\eta} \right) \tag{8}$$

where ρ_s is the density of solid particles (average 2.65 g/cm^3), ρ_f is the density of the fluid, g is the gravity acceleration, η is the viscosity of suspending fluid (0.01 g/cm.s), r is the equivalent spherical radius of falling particle $r = \sqrt{d^2/4}$.

Considering the particles' diameter and terminal velocity, Clay is representative in calculating the level of fine sediments. Sediment level prediction can be done using the Hans-Peter Kozerski approach, which follows the concept of the deep Westrich equation (Kozerski, 2002):

$$sed \ = \ C \ W_s^* \left(1 - \ V/V_{crit,sed}\right) \qquad (9)$$

where sed is the sediment rate (g/m^2.d), C is the concentration of suspended matter (g/m), W_s is the sinking velocity (m/d), V is the flow velocity (m/d), $V_{crit,sed}$ is the critical velocity for sedimentation (m/d) about 8.1 cm/d.

Meanwhile, for irregularly shaped sediment particles, the settling velocity, apart from being determined by density and size, is also influenced by the particles' shape and the fluid's viscosity, as shown in equation (10) (Zhu *et al.*, 2017).

$$W_s = \sqrt{\frac{2(\rho_s - \rho_f)gV}{\rho_f C_d A_p}} \qquad (10)$$

where g is the gravitational acceleration, V is the particle volume, A_p is the projected area of the body to flow direction perpendicular, ρ_s is the particle density, ρ_f is the fluid density, and C_d is the shape drag coefficient.

Several velocity equations for microplastic particles have been proposed by previous studies (Nguyen *et al.*, 2022; Sethulekshmi *et al.*, 2023; Stead & Bond, 2023; Yang *et al.*, 2023; Yu *et al.*, 2022; Zhang *et al.*, 2023).

2.3 The Impact of Sedimentation Rate on Coral Reefs

The direct impact of sediments on aquatic ecosystems is reduced lighting, intensity, faster light attenuation, reduced photosynthetic capacity, and smothering of coral polyps. Naturally, coral reefs can keep the surface clean of sediment particles to prevent sediment accumulation, suppressing the underlying tissue (Weber *et al.*, 2012). Corals need a relatively long time to clean the fine sediment particles (Bainbridge *et al.*, 2018), so it can cause constriction of polyps and damage to colonies, and it even has the potential to be the biggest destroyer of coral reefs (Erftemeijer *et al.*, 2012). Coral reefs' resilience to sedimentation exposure depends on the sediment accumulation rate (**Table 2**).

The recommended threshold value for silt-clay-sized sediments is 5–6 mg/cm^2.d (Li *et al.*, 2013). Under general conditions, a sediment level of ≥10 mg/cm^2.d is sufficient to endanger the vitality and health of corals (Loiola *et al.*, 2013; Rogers, 1990; Dutra *et al.*, 2006).

Damage to a particular coral colony network is related to the sedimentation rate and depends on the accompanying organic components (Fabricius, 2005). For an organic matter content of about 10% of the sediment content, a sediment rate of up to 15 mg/cm^2.d for 120 hours is sufficient to cause damage to coral (Loya, 1976). The daily maximum sedimentation rate must be watched if it reaches 15 mg/cm^2.d or the average annual rate is 3 mg/cm^2.d. Excessive coral mortality can occur if the concentration of suspended sediments is equivalent to an average of 1.6 mg/L in winter and 2.4 mg/L during the wet season and summer (Bartley *et al.*, 2014). The quantity of coral presence drops exponentially as the sedimentation rate increases. At sedimentation rates <10 mg/cm^2.d, the coral presence was almost three times greater than at rates between 10 and 50 mg/cm^2.d and almost 30 times more excellent when

rates were between 50 and 100 mg/cm^2.d. At a sediment rate >110 mg/cm^2.d , the presence of corals was not found (Minton *et al.*, 2022).

Table 2. Summary of studies measuring the effect of exposure to sedimentation on coral reefs refers to previous studies.

Exposure concentration	Exposure duration	Endpoint	Effect concentration and response	Species
2 – 12 mg/cm^2.d	8 months	Recruitment / Mortality	30% reduction in settlement and 60% reduction in recruit survival.	*Acropora millepora*
3 mg/cm^2.d	2 days	Recruitment	~84% reduction in recruitment on upper surfaces	*Acropora millepora*
8 mg/cm^2.d	2 days	Recruitment	~96% reduction in recruitment on upper surfaces	*Acropora millepora*
12 and 20 mg/cm^2.d without TEP ('marine snow')	43 h	Minor	0 and 4% recruit mortality, respectively	*Acropora willisae*
12 and 20 mg/cm^2.d with TEP ('marine snow')	43 h	Mortality	33 and 98% recruit mortality, respectively	*Acropora willisae*
>10 mg/cm^2.d	Long-term	Mortality / Community	Reduction in coral species richness, coral cover, coral growth rates, calcification, net productivity of corals, and reef accretion; increased proportion of branching forms. Species-specific capability for particle rejection and survival at lower light.	*(coral reef)*
33, 66, 100, 133 mg/cm^2.d	12, 20, 36 and 44 h of exposure	Physiological / mortality	Stress: decreased Fv/Fm and partial mortality. The severity of the effect increased with the amounts of organic contents and the amount and duration of exposure.	*Montipora peltiformis*
79 – 234 mg/cm^2.d	Up to 40 h	Physiological / mortality	The severity of the effect increased from photo physiological stress to partial mortality with increasing amount and duration of exposure.	*Montipora peltiformis*
50 – 200 mg/cm^2.d of 70/30% CaCO$_3$	6 days	Physiological	The effect depended on species, turbulence, and grain size, ranging from no effect to tissue bleaching.	*42 species*
200 mg/cm^2.d	Days	Mortality	Partial mortality: tissue necrosis	*Scleractinia and Alcyonacea*
200 – 300 mg/cm^2.d	Days to weeks	Physiological	Stress: decreased growth	*Acropora formosa*
430 mg/cm^2.d	>24 hr	Physiological	Stress: Reduce horizontal growth	*Acropora palmata, Acropora cervicornis, Porites astreoides, Agaricia agaricites*

Sedimentation can also be expressed in terms of the thickness of the accumulated sediment and is a valuable benchmark for conceptualizing deposition (Duckworth *et al.,* 2017). Assuming a wet bulk density of 1,050 kg/m^3 for freshly deposited sediments, a sedimentation rate of 8 mg/cm^2.d would result in a sediment layer only 80 μm thick. For sedimentation values of 5, 10, 25, 50, 100, and 250 mg/cm^2.d, it is predicted to produce a deposition thickness of 0.05, 0.11, 0.26, 0.53, 1.05, and 2.64 mm, respectively. A current carrying 12.6 t of sediment over an area of 2,314 m^2 in 6 days indicates that a very high percentage of this sediment was potentially deposited (5.2%) (Schlaefer *et al.,* 2022).

3. MATERIAL AND METHODS

This study combines experimental scale models and empirical approaches. The research object is the twin-propeller model of the Landing Craft Tank type of the Mini LNG Ship. The propeller data are available in **Figure 4** and **Table 3**.
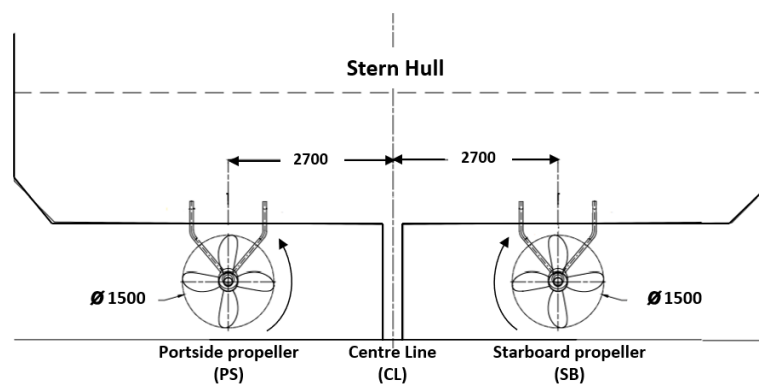
Figure 4. Propeller position at the stern hull of the ship.

Figure 4 shows the sketch of the twin propellers position at the ship stern, where the distance between the left and right propeller shafts to the center line of the ship is 2.7 m each so that the distance between the propeller shafts is 5.4 m or around 3.6 of propeller diameter (*Dp*). The propeller on the ship's right side is called the Starboard Propeller and rotates clockwise, and the Portside Propeller rotates anti-clockwise. The primary considerations in selecting a propeller rotation system are stability, seakeeping, and ship maneuvering.

Table 3. Propeller dimension *) Scale factor: 1:11.428.

Parameter	Symbol	Full scale	Model scale*	unit
Diameter	Dp	1.499	0.131	m
The pitch at the Diameter Ratio	P/Dp	1.144	1.144	
Expanded blade area ratio	A_E / A_0	0.400	0.400	
Numbers of blade	Z	4	4	blade

The initial stage is to investigate the velocity profile of the water flow velocity generated by the propeller's rotation in the hydrodynamics laboratory. Experimental data form the basis of an empirical approach to determine sedimentation potential. Next, an analysis and comparison of sediment potential and coral sensitivity to sedimentation was carried out to get an idea of the sedimentation rate and its effect on coral reef habitat.
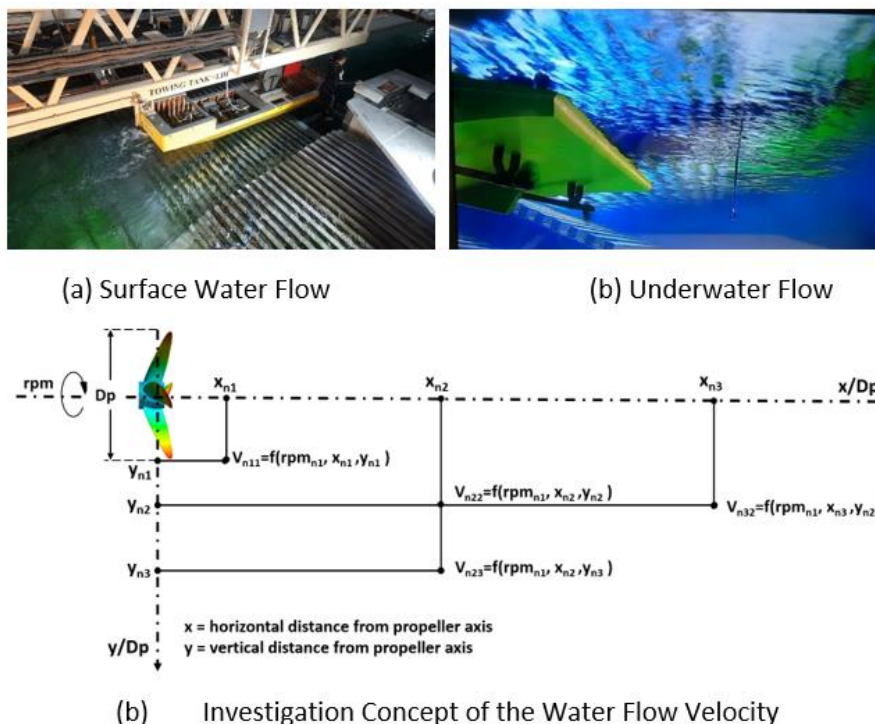
3.1.   Investigation of the Water Flow Velocity

The ship and propeller were each made into a scale model based on the data in **Table 3** for experimental purposes. The model was moved to the experimental tank for the hydrodynamics experimental installation system.

Figure 5(a) shows the ship model and propeller installed in the installation section of the experimental tank, with the model position facing the edge of the end of the tank. Meanwhile, the position of the propeller faces the central part of the experimental tank, where the bottom of the tank is equipped with a series of wave dampers.

Figure 5(b) shows the flow posture below the water surface, where the position of the flow velocity measuring instrument is installed at the back of the propeller. The experimental implementation has considered properties such as propeller Reynolds and water flow Reynolds numbers. For this experiment, the Reynolds number of the propeller is 6×10^7 greater than 7×10^4, and the Reynolds number of water flow is 5.3×10^6 greater than 3×10^3, for the condition that the effect of scale on viscosity can be ignored.

Figure 5(c) is a sketch of how to measure the speed of water flow from propeller rotation. Measurements were carried out at propeller rotations of 75 rpm, 120 rpm, 230 rpm, and 366 rpm. Each rpm was observed at 4 depths, namely $0.5Dp$, $1.0Dp$, $1.5Dp$, and $2.0Dp$ from the propeller rotation axis and horizontal distances of $1.5Dp$, $3.0Dp$, $4.5Dp$, $6.0Dp$, $7,5Dp$, and $9.0Dp$. Flow velocity was measured using a portable velocity meter with a 1 to 400 cm/s measurement range and an error rate of ≤1.5%.

(a) Surface Water Flow   (b) Underwater Flow

(b)   Investigation Concept of the Water Flow Velocity

Figure 5. Water flow velocity investigation method.

3.2.   Sedimentation Rate Calculation

In the initial stage, this research took four types of particles representing the sediment's fineness and roughness: Clay, Silt, Sand, and Gravel. Next, the scour dimensions and sedimentation posture are determined using Eqs. (2) to (5), and the size of the sediment volume is based on Eqs. (6) and (7). The particle size of the seabed was used as the basis for the investigation, referring to **Table 4** (Ye *et al.*, 2011).

Table 4. Variation in the diameter of the seabed particle in (mm).

Particle	Fine	Medium	Coarse
Clay		< 0.002	
Silt	0.002–0.006	0.006–0.02	0.02–0.0625
Sand	0.0625–0.2	0.2–0.6	0.6–2.0
Gravel	2.0–6.0	6.0–20	20–60
Cobbles		>60	

The concentration of suspended material is obtained from the total weight of floating sediment M (g) divided by the volume it holds Vl (m^3). Determination of the sedimentation rate was carried out in 13 water column volume scenarios of 50 to 650 m^3, each with an additional interval of 50 m^3. For each volume scenario, the sedimentation rate was investigated in 4 rpm and four variations of y/Dp depth conditions. For the maximum sedimentation rate, the value of the current velocity V in equation (9) is taken to be close to zero.

Figure 6 illustrates how the propeller rotation causes scour and sedimentation on the bottom of the water. Large sediment particles immediately settle, while small floating sediment particles can spread further to cover the area around the coast and settle to cover the bottom of the surrounding waters. When the water flow from the propeller rotation erodes the bottom of the water, the concentration of suspended sediment will concentrate around the bottom and decrease towards the water's surface and further away from the propeller (Hong *et al.*, 2016). Approximately 97-98% of the volume of eroded sediment is deposited as piles of sediment around the scour hole, and around 2-3% will be carried away by the current in the form of floating sediment. The spread of floating sediment depends on the current speed or wave and will eventually settle to cover the surrounding aquatic ecosystem.
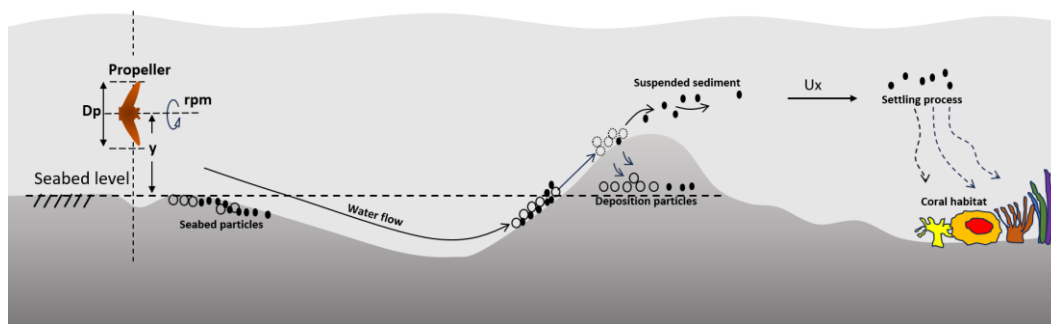
Figure 6. Sketch of erosion and sediment deposition processes.

4. RESULT AND DISCUSSION
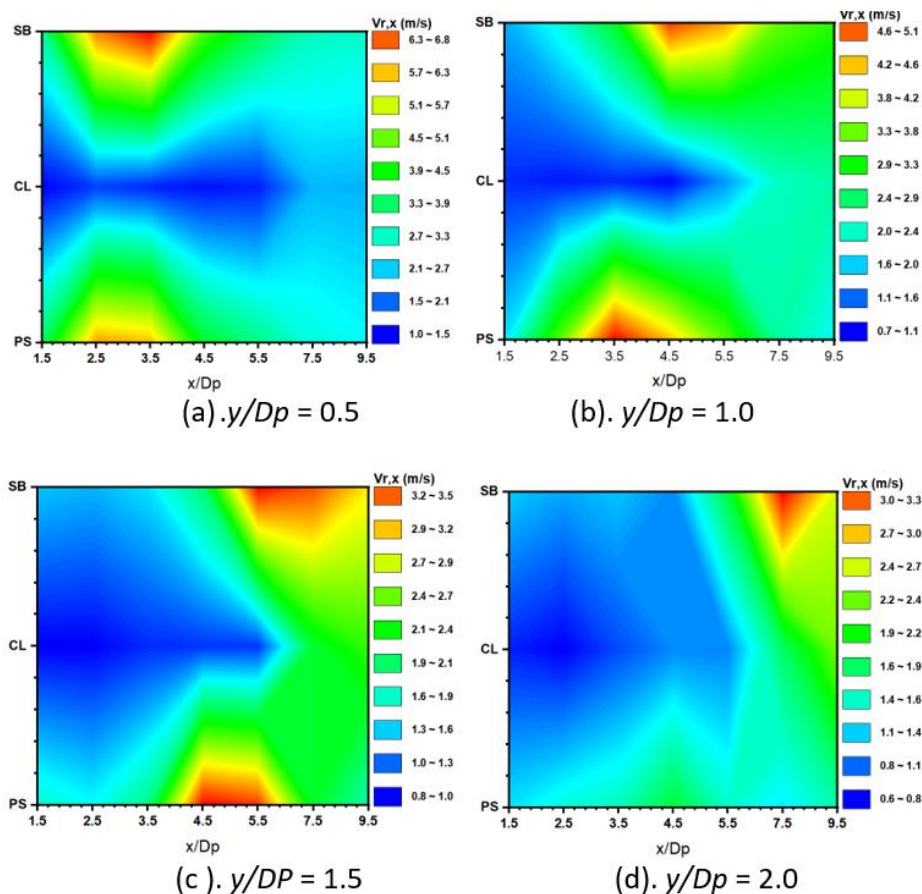### 4.1. Water Flow Velocity Posture

The measurement results from the model experiment show that the value of water flow velocity due to propeller rotation is significant at 366 rpm for all depth values of y/Dp. The speed value reaches 6,610 at a depth value of y/Dp=0.5, 4.841 m/s at a depth position of y/Dp=1.0, 3.311 m/s at a depth of y/Dp=1.5 and 3.193 m/s at y/Dp =2.0. The maximum flow velocity values for 75, 120, and 230 rpm rotation occur at a depth value of y/Dp=0.5 with respective values of 1.480, 2.280, and 4.160 m/s, as shown in **Table 5**. The distribution of speed values forms a flow velocity posture, as depicted in **Figure 7**, where the flow velocity value increases with increasing rpm and the closer the position is to the propeller axis.

Table 5. Water flow velocity (*Uo*).

	rpm			
y/Dp	75	120	230	366
	Uo (m/s)			
0.5	1.480	2.280	4.160	6.610
1.0	1.128	1.616	2.869	4.841
1.5	0.978	1.425	2.207	3.311
2.0	0.953	1.244	1.834	3.193

Figure 7(a) is the posture of the water flow velocity from the propeller rotation at a depth ratio of *y/Dp*=0.5. The maximum water flow velocity occurs in the Starboard Propeller (*SB*) and Portside Propeller (*PS*) axes at a horizontal distance ratio *x/Dp* between 2.5 and 3.5. Meanwhile, the speed of water flow on the center line (*CL*) axis has yet to occur significantly.

Figure 7(b) is the flow velocity posture at the depth ratio *y/Dp*=1.0. Maximum flow velocity occurs at a horizontal distance ratio between 3.5 and 5.5. The flow velocity on the Center Line (*CL*) axis has begun to increase significantly.

(a) .*y/Dp* = 0.5   (b). *y/Dp* = 1.0

(c). *y/DP* = 1.5   (d). *y/Dp* = 2.0

Figure 7. The water flow velocity posture for propeller rotation at 366 rpm.

Figure 7(c) represents the water flow posture of the propeller rotation at a depth ratio of *y/Dp*=1.5, where the maximum speed occurs at a ratio of *x/Dp* > 6.5, and the flow speed on the center axis (*CL*) increases significantly.

Figure 7(d) is the water flow velocity posture at a depth ratio *y/Dp*=2.0, where the maximum velocity occurs at a horizontal distance ratio *x/Dp* > 7.5, and the flow velocity at the center line also increases.

From the visible water flow velocity posture up to a distance of *x/Dp* 6.5, the flow velocity for all depths still occurs on each propeller's axis. This phenomenon is characteristic of the *ECRTP* system, where the maximum speed of water flow along each propeller axis will decrease as the horizontal distance from the propeller increases. Conversely, the flow velocity at the center line will increase (Kadir *et al.*, 2023). It is also reinforced by the tendency that the maximum depth of seabed scour due to *ECRTP* occurs along the rotation axis of each propeller (Cui *et al.*, 2020).

4.2. Sedimentation Volume

The volume of sediment that arises is calculated by Eqs. (2) to (7) at varying depths of *y/Dp*=0.5, *y/Dp*=1.0, *y/Dp*=1.5, and *y/Dp*=2.0 for four types of seabed particles Clay, Silt, Sand, and Gravel. **Figure 8** is the achievement of volume values for the seabed particle type. The maximum volume for each type of particle is achieved at *y/Dp*=0.5, and the propeller rotation is 366 rpm with the values achieved for Clay particles of 47.64 m^3, Mud of 42.71 m^3, Sand of 36.34 m^3 and Gravel of 34.32 m^3. Meanwhile, the minimum volume is achieved at *y/Dp*=2.0 and a propeller rotation of 75 rpm, namely 1.53 m^3 for Clay particles, 1.37 m^3 for Silt, 1.17 m^3 for Sand, and 1.1 m^3 for Gravel.

Reducing the propeller rotation from 366 to 230 rpm has implications for reducing the average sediment volume by 74%; from 230 to 120 rpm, there is a decrease of 80%, and from 120 to 75 rpm, there is a decrease of 72%. On the other hand, under constant rpm conditions, increasing the depth value from *y/Dp*= 0.5 to *y/Dp*=1.0 has implications on decreasing the average sediment volume by 79%, while there is a volume reduction of 79% when increasing the depth value from *y/Dp*=1.0 to *y/Dp*=1.5, and the reduction of 31% when increasing one from *y/Dp*=1.5 to *y/Dp*=2.0. These results show that the amount of floating sediment that occurs will decrease significantly as the propeller distance to the bottom of the water increases and the propeller rotation itself decreases. This phenomenon is in line with seabed scouring as a source of sedimentation caused by propeller rotation (Penna *et al.*, 2019).

The discussion focuses more on fine sediment, considering corals need a relatively long time to clean fine sediment particles (Bainbridge *et al.*, 2018). Apart from that, the scope of distribution of fine sediment will be broader than coarse particles such as Sand and Gravel. The floating sediment weight is obtained by multiplying the volume *Vs* with the density ρ_s, as shown in **Table 6**.
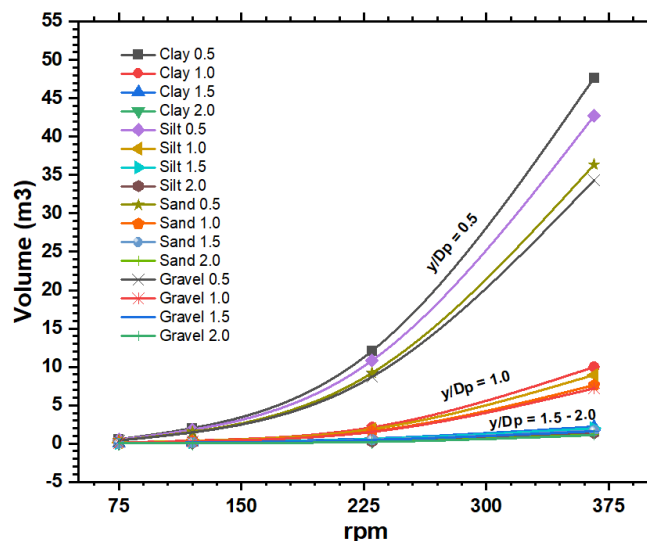

Figure 8. Suspended sediment volume curve caused by propeller rotation.

Table 6. Sediment mass of floating clay particles.

y/Dp	rpm			
	75	120	230	360
	M (g)			
0.5	1,474	5,337	31,1994	126,251
1.0	348	1,012	5,580	26,437
1.5	59	181	664	2,219
2.0	42	93	294	1,528

4.3. Determining Sedimentation Rate

The sedimentation rate is expressed in the number of grams of weight of sediment particles per square cm in one day (mg/cm^2.d). With the same volume of sediment particles, the sedimentation rate will be greater in a small water column volume distribution than if the sediment particles cover a large area of the water column. The complete calculation results are given in **Figure 9**.

(a) *y/Dp*=0.5 (b). *y/Dp*=1.0

(c). *y/Dp*=1.5 (d). *y/Dp*=2.0
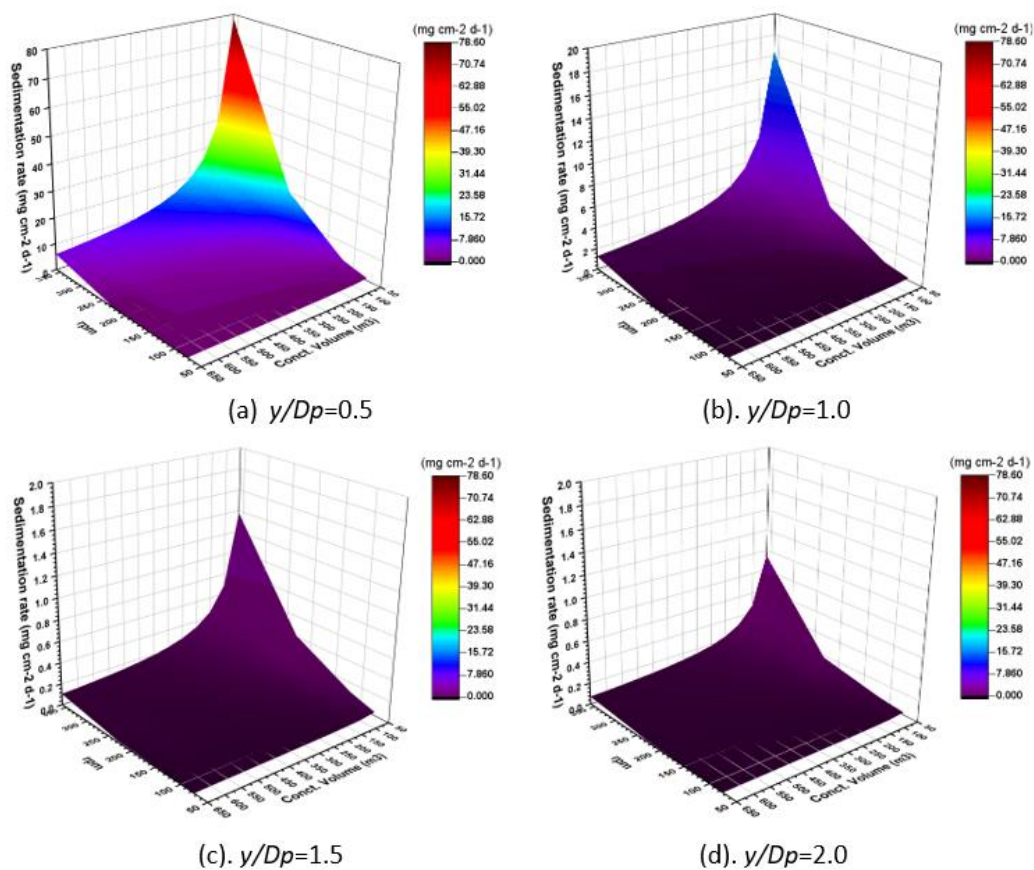
Figure 9. Sedimentation rate prediction.

Figure 9(a) shows the distribution of sedimentation rate at the depth ratio *y/Dp*=0.5 for all propeller rpm values. In this position, there are two conditions where the sedimentation rate is above the coral reef threshold (10 mg/cm^2.d). The first is the water column volume scenario of 50 to 100 m^3 for a propeller rotation of 230 rpm, and the second is the water column volume scenario of 50 to 400 m^3 for a propeller rotation of 360 rpm. The maximum sedimentation rate achieved was 78.5 mg/cm^2.d. If compared with the description in **Table 2**

in Section 2.3, it can be concluded that the sedimentation rate at *y/Dp*=0.5 can damage coral species such as Acropora Millenopora, Coral Reef, Montipora Peltiformis, and 45 other types.

Figure 9(b) depicts the sedimentation rate at the depth ratio *y/Dp*=1.0. In this condition, one scenario produces a sedimentation rate of more than 10 mg/cm^2.d, namely in the scenario of a water column volume of 50 m^3 with a propeller rotation of 360 rpm. The resulting sedimentation rate is 16,432 mg/cm^2.d. Thus, it can disrupt the life of Acropora Millenopora and Coral Reef coral species.

Figure 9(c) depicts the sedimentation rate at a depth of *y/Dp*=1.5 where the maximum value of the sedimentation rate only reaches 1,379 mg/cm^2.d in the 50 m^3 water column scenario with 360 rpm. **Figure 9(d)** is the sedimentation rate at *y/Dp*=2.0 where in this condition the achieved value is less than 1 mg/cm^2.d for all water column volume scenarios. From these achievement values, these two conditions are safe for the coastal waters ecosystem.

Figure 10 is a curve of the propeller rotation threshold against the depth-to-propeller diameter ratio. This graph results from an approach to represent the calculation results of several variations in propeller rotation, distance from the propeller axis to the bottom of the water, and variations in sediment volume distribution scenarios. The blue line trend shows that propeller rotation of 100 to 250 rpm is prone to causing environmental disturbances, so the minimum distance between the propeller rotation axis and the base must be strictly observed. At a ratio of *y/Dp* = 2.0, an increase in propeller rotation does not significantly affect the aquatic environment. The curve equation is given in **Table 7**.
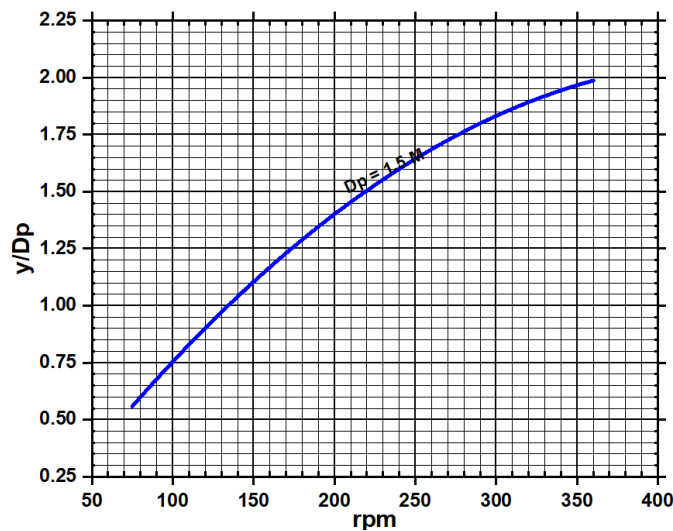

Figure 10. Propeller rotation threshold curve for coral reef ecosystem (*Dp*=1.5 M).

Table 7. Propeller rotation threshold curve equation.

Variable	Notation / Value
Equation	*y* = Intercept + *B1x*+ *B2x*^{2}
Plot	*y/Dp*
Weight	No Weighting
Intercept	-0.10796 ± 0.29789
B1	0.0097 ± 0.00337
B2	-1.07916. 10^{-5} ± 7.58411. 10^{-6}
Residual Sum of Squares	0.01626
R-Square (*COD*)	0.98699
Adj. R-Square	0.96097

5. CONCLUSION

Uncontrolled rotation of ship propellers can have a severe impact on aquatic ecosystems. The variables that determine the level of disturbance to the environment are the diameter of the propeller, the rotation of the propeller, the Seabed particles, and the distance of the propeller to the seabed. In a twin-propeller system, the erosion and sedimentation posture of the seabed varies according to the rotation of the propeller used. Twin propellers with a diameter (Dp) = 1.5 m can trigger a sedimentation rate of up to 19.886 mg/cm^2.d if they rotate more than 120 rpm at a propeller axis position of 0.5Dp above the seabed. Likewise, if the propeller rotates more than 230 rpm at a propeller axis distance of 1.0Dp above the seabed, it can trigger a sedimentation rate of up to 16.4 mg/cm^2.d and damage coral reefs. Meanwhile, propeller rotation does not significantly impact coral reef habitat if the propeller rotation axis is in a position of 1.5Dp to 2.0Dp above the seabed. Further research needs to be done on various sizes and types of propellers.

6. ACKNOWLEDGMENT

7. AUTHORS' NOTE

The authors declare that there is no conflict of interest regarding the publication of this article. The authors confirmed that the data and the paper are free of plagiarism.

8. REFERENCES

Al Husaeni, D. F., and Nandiyanto, A. B. D. (2022). Bibliometric using vosviewer with publish or perish (using Google Scholar data): From step-by-step processing for users to the practical examples in the analysis of digital learning articles in pre and post covid-19 pandemic. *ASEAN Journal of Science and Engineering*, *2*(1), 19–46.

Bainbridge, Z., Lewis, S., Bartley, R., Fabricius, K., Collier, C., Waterhouse, J., Garzon-Garcia, A., Robson, B., Burton, J., Wenger, A., and Brodie, J. (2018). Fine sediment and particulate organic matter: A review and case study on ridge-to-reef transport, transformations, fates, and impacts on marine ecosystems. *Marine Pollution Bulletin*, *135*, 1205–1220.

Bartley, R., Bainbridge, Z. T., Lewis, S. E., Kroon, F. J., Wilkinson, S. N., Brodie, J. E., and Silburn, D. M. (2014). Relating sediment impacts on coral reefs to watershed sources, processes and management: A review. *Science of the Total Environment*, *468–469*, 1138–1153.

Ceccarelli, D. M., Lestari, A. P., Rudyanto, and White, A. T. (2022). Emerging marine protected areas of eastern Indonesia: Coral reef trends and priorities for management. *Marine Policy*, *141*, 105091.

Cui, Y., Lam, W. H., Robinson, D., and Hamill, G. (2020). Temporal and spatial scour caused by external and internal counter-rotating twin-propellers using Acoustic Doppler

Velocimetry. *Applied Ocean Research*, *97*, 102093.

Cui, Y., Lam, W. H., Zhang, T., Sun, C., and Hamill, G. (2019). Scour induced by single and twin propeller jets. *Water (Switzerland)*, *11*(5), 1097.

Cui, Y., Lam, W. H., Zhang, T., Sun, C., Robinson, D., and Hamill, G. (2019a). Temporal model for ship twin-propeller jet induced sandbed scour. *Journal of Marine Science and Engineering*, *7*(10), 339.

Curulli, G., Llull, T., Penna, N., Mujal-Colilles, A., Gironella, X., Sánchez-Arcilla, A., and Gaudio, R. (2022). Relationship between eroded volume and main scour hole dimensions near quay walls caused by internal counter-rotating twin-propellers. *Ocean Engineering*, *259*, 111744.

Curulli, G., Penna, N., and Gaudio, R. (2023). Improved formulation for the geometric characteristics of the scour hole and deposition mound caused by a rotating propeller jet on a mobile bed. *Ocean Engineering*, *267*, 113175.

Duckworth, A., Giofre, N., and Jones, R. (2017). Coral morphology and sedimentation. *Marine Pollution Bulletin*, *125*(1–2), 289–300.

Dutra, L. X. C., Kikuchi, R. K. P., and Leão, Z. M. A. N. (2006). Effects of sediment accumulation on reef corals from Abrolhos, Bahia ,Brazil. *Journal of Coastal Research*, *22*, 633–638.

Erftemeijer, P. L. A., Riegl, B., Hoeksema, B. W., and Todd, P. A. (2012). Environmental impacts of dredging and other sediment disturbances on corals: A review. *Marine Pollution Bulletin*, *64*(9), 1737–1765.

Fabricius, K. E. (2005). Effects of terrestrial runoff on the ecology of corals and coral reefs: Review and synthesis. *Marine Pollution Bulletin*, *50*(2), 125–146.

Fiandini, M., Bayu, A., Nandiyanto, D., Fitria, D., Husaeni, A., Novia, D., and Mushiban, M. (2024). How to calculate statistics for significant difference test using SPSS: Understanding students comprehension on the concept of steam engines as power plant how to calculate statistics for significant difference test using SPSS. *Indonesian Journal of Science and Technology*, *9*(1), 45–108.

Flynn, R. L., and Forrester, G. E. (2019). Boat anchoring contributes substantially to coral reef degradation in the British Virgin Islands. *PeerJ*, *7*, e7010.

Forrester, G. E. (2020). The influence of boat moorings on anchoring and potential anchor damage to coral reefs. *Ocean and Coastal Management*, *198*, 105354.

Guarnieri, A., Saremi, S., Pedroncini, A., Jensen, J. H., Torretta, S., Vaccari, M., and Vincenzi, C. (2021). Effects of marine traffic on sediment erosion and accumulation in ports: A new model-based methodology. *Ocean Science*, *17*(2), 411–430.

Hong, J.-H., Chiew, Y.-M., Hsieh, S.-C., Cheng, N.-S., and Yeh, P.-H. (2016). Propeller jet–induced suspended-sediment concentration. *Journal of Hydraulic Engineering*, *142*(4), 04015064.

Kadir, A., Subagio, A., Kartikasari, D., Sadiah, S., Himawan, S., Virliani, P., Kusuma, Y. F., Satria, E., Putra, A., and Eritha, F. N. (2023). The effect of the external counter rotating for the water flow velocity profile of twin propeller system. *Journal of Applied Science and*

Engineering, *27*(8), 2945–2955.

Kaidi, S., Smaoui, H., and Sergent, P. (2021). Numerical investigation of the inland transport impact on the bed erosion and transport of suspended sediment: Propulsive system and confinement effect. *Journal of Marine Science and Engineering*, *9*(7), 746.

Kozerski, H. P. (2002). Determination of areal sedimentation rates in rivers by using plate sediment trap measurements and flow velocity - Settling flux relationship. *Water Research*, *36*(12), 2983–2990.

Li, X. bao, Huang, H., Lian, J. sheng, Liu, S., Huang, L. min, and Yang, J. hui. (2013). Spatial and temporal variations in sediment accumulation and their impacts on coral communities in the Sanya Coral Reef Reserve, Hainan, China. *Deep-Sea Research Part II: Topical Studies in Oceanography*, *96*, 88–96.

Loiola, M., Oliveira, M. D. M., and Kikuchi, R. K. P. (2013). Tolerance of Brazilian brain coral Mussismilia braziliensis to sediment and organic matter inputs. *Marine Pollution Bulletin*, *77*(1–2), 55–62.

Loya, Y. (1976). Effects of water turbidity and sedimentation on the community structure of puerto rican corals. *Bulletin of Marine Science*, *26*(4), 450–466.

Minton, D., Burdick, D., and Brown, V. (2022). Changes in coral reef community structure along a sediment gradient in Fouha Bay, Guam. *Marine Pollution Bulletin*, *181*, 113816.

Nandiyanto, A. B. D., and Al Husaeni, D. F. (2021). A bibliometric analysis of materials research in Indonesian journal using VOSviewer. *Journal of Engineering Research (Kuwait)*, *9*, 1–16.

Nguyen, T. H., Kieu-Le, T. C., Tang, F. H. M., and Maggi, F. (2022). Controlling factors of microplastic fibre settling through a water column. *Science of the Total Environment*, *838*(December 2021), 156011.

Penna, N., D'Alessandro, F., Gaudio, R., and Tomasicchio, G. R. (2019). Three-dimensional analysis of local scouring induced by a rotating ship propeller. *Ocean Engineering*, *188*, 106294.

Razak, T. B., Boström-Einarsson, L., Alisa, C. A. G., Vida, R. T., and Lamont, T. A. (2022). Coral reef restoration in Indonesia: A review of policies and projects. *Marine Policy*, *137*, 104940.

Rogers, C. S. (1990). Responses of coral reefs and reef organisms to sedimentation. *Marine Ecology Progress Series Oldendorf*, *62*(1), 185-202.

Rogers, Caroline S. (1990). Responses of coral reefs and reef organisms to sedimentation. *Marine Ecology Progress Series*, *62*, 185–202.

Ryan, K. E., Walsh, J. P., Corbett, D. R., and Winter, A. (2008). A record of recent change in terrestrial sedimentation in a coral-reef environment, La Parguera, Puerto Rico: A response to coastal development? *Marine Pollution Bulletin*, *56*(6), 1177–1183.

Schlaefer, J. A., Tebbett, S. B., Bowden, C. L., Collins, W. P., Duce, S., Hemingson, C. R., Huertas, V., Mihalitsis, M., Morais, J., Morais, R. A., Siqueira, A. C., Streit, R. P., Swan, S., Valenzuela, J., and Bellwood, D. R. (2022). A snapshot of sediment dynamics on an inshore coral reef. *Marine Environmental Research*, *181*, 105763.

Scully, B., and Young, D. (2021). Evaluating the underkeel clearance of historic vessel transits in the southwest pass of the mississippi river. *Journal of Waterway, Port, Coastal, and Ocean Engineering*, *147*(5), 1–13.

Sethulekshmi, S., Kalbar, P., and Shriwastav, A. (2023). A unified modelling framework for type I (discrete) settling and rising of microplastics in primary sedimentation tanks. *Journal of Environmental Management*, *334*, 117444.

Soegoto, H., Soegoto, E. S., Luckyardi, S., and Rafdhi, A. A. (2022). A bibliometric analysis of management bioenergy research using vosviewer application. *Indonesian Journal of Science and Technology*, *7*(1), 89–104.

Stead, J. L., and Bond, T. (2023). The impact of riverine particles on the vertical velocities of large microplastics. *Science of the Total Environment*, *896*, 165339.

Tan, R. İ., and Yüksel, Y. (2018). Seabed scour induced by a propeller jet. *Ocean Engineering*, *160*, 132–142.

Van Rijn, L. C. (2007). Unified view of sediment transport by currents and waves. III: Graded beds. *Journal of Hydraulic Engineering*, *133*(7), 761-775.

Victor, S., Neth, L., Golbuu, Y., Wolanski, E., and Richmond, R. H. (2006). Sedimentation in mangroves and coral reefs in a wet tropical island, Pohnpei, Micronesia. *Estuarine, Coastal and Shelf Science*, *66*(3–4), 409–416.

Weber, M., De Beer, D., Lott, C., Polerecky, L., Kohls, K., Abed, R. M. M., Ferdelman, T. G., and Fabricius, K. E. (2012). Mechanisms of damage to corals exposed to sedimentation. *Proceedings of the National Academy of Sciences of the United States of America*, *109*(24), E1558-E1567.

Yang, G., Yu, Z., Baki, A. B. M., Yao, W., Ross, M., Chi, W., and Zhang, W. (2023). Settling behaviors of microplastic disks in water. *Marine Pollution Bulletin*, *188*, 114657.

Ye, Z., Cheng, L., and Zang, Z. (2011). Experimental study of erosion threshold of reconstituted sediments. *Proceedings of the International Conference on Offshore Mechanics and Arctic Engineering - OMAE*, *7*, 973–983.

Ytreberg, E., Åström, S., and Fridell, E. (2021). Valuating environmental impacts from ship emissions–The marine perspective. *Journal of Environmental Management*, *282*, 111958.

Yu, Z., Yang, G., and Zhang, W. (2022). A new model for the terminal settling velocity of microplastics. *Marine Pollution Bulletin*, *176*, 113449.

Zhang, J., Ji, C., Liu, G., Zhang, Q., and Xing, E. (2023). Settling processes of cylindrical microplastics in quiescent water: A fully resolved numerical simulation study. *Marine Pollution Bulletin*, *194*(PB), 115438.

Zhu, X., Zeng, Y. H., and Huai, W. X. (2017). Settling velocity of non-spherical hydrochorous seeds. *Advances in Water Resources*, *103*, 99–107.